2. Adam, G. & Gibbs, J. H. On the temperature dependence of cooperative relaxation properties in glass forming liquids. *J. Chem. Phys.* **43,** 139–146 (1965).
3. Weeks, E. R., Crocker, J. L., Levitt, A. C., Schofield, A. & Weitz, D. A. Three-dimensional direct imaging of structural relaxation near the colloidal glass transition. *Science* **287,** 627–629 (2000).
4. Bennemann, C., Donati, C., Baschnagel, J. & Glotzer, S. C. Growing range of correlated motion in a polymer melt on cooling towards the glass transition. *Nature* **399,** 246–249 (1999).
5. Binder, K., Baschnagel, J., Kob, W. & Paul, W. Glass physics: still not transparent. *Phys. World* **12,** 54 (1999).
6. Tracht, U. *et al.* Length scale of dynamic heterogeneities at the glass transition determined by multidimensional nuclear magnetic resonance. *Phys. Rev. Lett.* **81,** 2728–2731 (1998).
7. Schiener, B., Bohmer, R., Loidl, A. & Chamberlin, R. V. Nonresonant spectral hole burning in the slow dielectric response of supercooled liquids. *Science* **274,** 752–754 (1996).
8. Bohmer, R. *et al.* Nature of the nonexponential primary relaxation in structural glasses probed by dynamically selective experiments. *J. Non-Cryst. Solids* **235,** 1–8 (1998).
9. Ediger, M. D. Spatially heterogeneous dynamics in supercooled liquids. *Annu. Rev. Phys. Chem.* **51,** (in the press).
10. Dixon, P. K., Wu, L., Nagel, S. R., Williams, B. D. & Carini, J. P. Scaling in the relaxation of a supercooled liquid. *Phys. Rev. Lett.* **65,** 1108–1111 (1990).
11. Arbe, A., Colmenero, J., Monkenbusch, M. & Richter, D. Dynamics of glass forming polymers: "homogeneous" vs. "heterogeneous" scenario. *Phys. Rev. Lett.* **81,** 590–593 (1998).
12. Grigera, T. S. & Israeloff, N. E. Observation of fluctuation-dissipation-theorem violations in a structural glass. *Phys. Rev. Lett.* **83,** 5038–5041 (1999).
13. Martin, Y., Abraham, D. W. & Wickramasinghe, H. K. High-resolution capacitance measurement and potentiometry by force microscopy. *Appl. Phys. Lett.* **52,** 1103–1105 (1988).
14. Walther, L. E., Israeloff, N. E., Vidal Russell, E. & Alvarez Gomariz, H. Mesoscopic scale dielectric relaxation at the glass transition. *Phys. Rev. B* **57,** R15112–R15115 (1998).
15. Vidal Russell, E., Walther, L. E., Israeloff, N. E. & Alvarez Gomariz, H. Nanometer scale dielectric fluctuations at the glass transition. *Phys. Rev. Lett.* **81,** 1461–1464 (1998).
16. Walther, L. E., Vidal Russell, E., Israeloff, N. E. & Alvarez Gomariz, H. Atomic force measurement of low frequency dielectric noise. *Appl. Phys. Lett.* **72,** 3223–3226 (1998).
17. Albrecht, T. R., Grütter, P., Horne, D. & Rugar, D. Frequency modulation detection using high-Q cantilevers for enhanced force microscope sensitivity. *J. Appl. Phys.* **69,** 668–673 (1991).
18. Forrest, J. A., Dalnoki-Veress, K., Stevens, J. R. & Dutcher, J. R. Effect of free surfaces on the glass transition temperature of thin polymer films. *Phys. Rev. Lett.* **77,** 2002–2005 (1996).
19. McCrum, N. G., Read, B. E. & Williams, G. *Anelastic And Dielectric Effects In Polymeric Solids* 302–305 (Dover, New York, 1991).
20. Tracht, U., Heuer, A., Spiess, H. W. Geometry of reorientational dynamics in supercooled poly(vinyl acetate) studied by 2D NMR echo experiments. *J. Phys. Chem.* **111,** 3720–3727 (1999).
21. Xia, X. & Wolynes, P. G. Fragilities of liquids predicted from the random first order transition theory of glasses. *Proc. Natl Acad. Sci. USA* **97,** 2990–2994 (2000).
22. Wang, J. & Wolynes, P. Intermittency of single molecule reaction dynamics in fluctuating environments. *Phys. Rev. Lett.* **74,** 4317–4320 (1995).

Acknowledgements

This research was supported by the NSF Division of Materials Research, and the Petroleum Research Fund administered by the American Chemical Society. We thank M. D. Ediger for helpful discussions and K. Sinnathamby for assistance.

Correspondence and requests for materials should be addressed to N.E.I. (e-mail: Israeloff@neu.edu).

Evidence for decoupling of atmospheric CO_2 and global climate during the Phanerozoic eon

Ján Veizer*, Yves Godderis† & Louis M. François†

** Institut für Geologie, Mineralogie und Geophysik, Ruhr Universität, 44780 Bochum, Germany, and Ottawa-Carleton Geoscience Centre, University of Ottawa, Ottawa, ON K1N 6N5, Canada*
† Laboratoire de Physique Atmosphérique et Planétaire, Université de Liège, 4000 Liège, Belgium

Atmospheric carbon dioxide concentrations are believed to drive climate changes from glacial to interglacial modes[1], although geological[1–3] and astronomical[4–6] mechanisms have been invoked as ultimate causes. Additionally, it is unclear[7,8] whether the changes between cold and warm modes should be regarded as a global phenomenon, affecting tropical and high-latitude temperatures alike[9–13], or if they are better described as an expansion and contraction of the latitudinal climate zones, keeping equatorial temperatures approximately constant[14–16]. Here we present a reconstruction of tropical sea surface temperatures throughout the Phanerozoic eon (the past ~550 Myr) from our database[17] of oxygen isotopes in calcite and aragonite shells. The data indicate large oscillations of tropical sea surface temperatures in phase with the cold–warm cycles, thus favouring the idea of climate variability as a global phenomenon. But our data conflict with a temperature reconstruction using an energy balance model that is forced by reconstructed atmospheric carbon dioxide concentrations[18]. The results can be reconciled if atmospheric carbon dioxide concentrations were not the principal driver of climate variability on geological timescales for at least one-third of the Phanerozoic eon, or if the reconstructed carbon dioxide concentrations are not reliable.

Calculated partial pressures of CO_2 in the atmosphere[18–20] (pCO_2) are indeed relatively low for the Permo/Carboniferous and Cenozoic icehouse episodes[1], times of predominantly cold climates lasting tens of millions of years[2], but for the other two Phanerozoic icehouses—the late Ordovician/earliest Silurian and the late Jurassic/early Cretaceous—all global biogeochemical models[19,20] predict high pCO_2 levels. In an attempt to resolve this discrepancy, particularly for the late Ordovician glaciation(s), theoretical models advocating the development of permanent high-latitude ice sheets[21] at more than 10 times present-day CO_2 levels have been proposed. As an alternative, we present here experimental evidence that suggests large variations in tropical sea surface temperatures (SSTs; up to 9 °C) between the peaks of greenhouse/icehouse modes.

The testing of model predictions on Phanerozoic timescales has been hampered by the lack of high-resolution isotope databases for ancient sea water, as reflected in (bio)chemical sediments. This has been particularly the case for oxygen isotopes, where the depletion in ^{18}O for progressively older sediments was mostly considered to be a product of post-depositional diagenetic overprint. However, new databases have been published[17] recently—based on ~4,500 low-Mg calcitic and 125 aragonitic shells—for $\delta^{18}O$, $\delta^{13}C$ and $^{87}Sr/^{86}Sr$, establishing the baseline for Phanerozoic $\delta^{18}O$ (Fig. 13 in ref. 17). Most studied samples originate from the photic zone of palaeotropical seas (30 °S–30 °N). The entire datasets are available at http://www.science.uottawa.ca/geology/isotope_data. Reference 17, because of the huge number of measurements, dealt only with the documentation of data and their quality, and with the arguments for the primary nature of the $\delta^{18}O$ record.

The secular trend for the $\delta^{18}O$ values of Phanerozoic carbonates, Fig. 13 in ref. 17, consists of a long-term rising linear trend that exceeds the duration of planetary greenhouse/icehouse modes. This trend is tectonically controlled, a proposition supported by the strong correlation of $\delta^{18}O$ with the $^{87}Sr/^{86}Sr$ signal for the Phanerozoic sea water (Figs 16 and 17 in ref. 17). Sr isotopes are a proxy for terrestrial tectonic processes, because seawater $^{87}Sr/^{86}Sr$ is controlled principally by inputs of Sr from rivers (weathering of ^{87}Sr-enriched continental crust) and from hydrothermal circulation cells at mid-ocean ridges (interaction with ^{87}Sr-depleted basalts). Such long-term tectonic signals have to be subtracted from the superimposed higher-order oscillations before any discussion of climatic consequences, and we therefore detrend the data by removing the least-squares linear fit.

The first-order $\delta^{18}O$ oscillations around the least-squares fit correlate well with the palaeoclimate as established from sedimentological criteria[1]. The icehouses usually coincide with ^{18}O-enriched values and greenhouses with ^{18}O-depleted values (Fig. 1). We propose therefore that the Phanerozoic $\delta^{18}O$ oscillations reflect variations in SSTs. Future improvements on the Phanerozoic database may result in amelioration of the amplitudes, or in partial temporal shifts of some of the peaks. This is particularly the case for the Neogene interval, where the running mean is forced to higher values by the inclusion of some isotopically heavy planktonic

foraminifera from the Northern Pacific Ocean. Subsequently, the running mean declines sharply to modern values for tropical calcite. Nonetheless, considering the size and quality of this database, it is unlikely that any future refinements will unravel the overall correlation between palaeoclimate and $\delta^{18}O$.

The proposition that the detrended $\delta^{18}O$ oscillations reflect climatically controlled SSTs is also supported by a correlation with the palaeolatitudinal distribution of ice-rafted debris (PIRD) as a function of geological age[22] (Fig. 1). In this study, all data were re-calibrated to the timescale of ref. 23. At first, a simple statistical analysis that was based on the detrended $\delta^{18}O$ (running mean at 10/50 Myr; see Fig. 1 legend for nomenclature) and on the PIRD signal interpolated every 10 Myr at extant PIRD (29 points, with intervals without ice-rafted debris removed from the analysis), yielded only a mediocre correlation coefficient (0.55). This is not surprising, considering the coarse time resolution of the PIRD database compared to the $\delta^{18}O$ signal. We then performed a decomposition in Fourier series of the detrended $\delta^{18}O$ and PIRD signals. Both series display a dominant component at ~135 Myr, regardless of the resolution adopted for the $\delta^{18}O$ signal (Fig. 2). Thus the result is not dependent on the parameters, such as window size and time-step, that were adopted for the running mean procedure. The maximal calculated dephasing between the two signals is 9 Myr, which is not significant considering the coarse resolution of the PIRD. The coherence, a measure of correlation between two periodic signals, is 0.92. This correlation between past global climate and the detrended $\delta^{18}O$ signal is further corroborated by the frequency histograms of other glacial deposits (OGD), at present

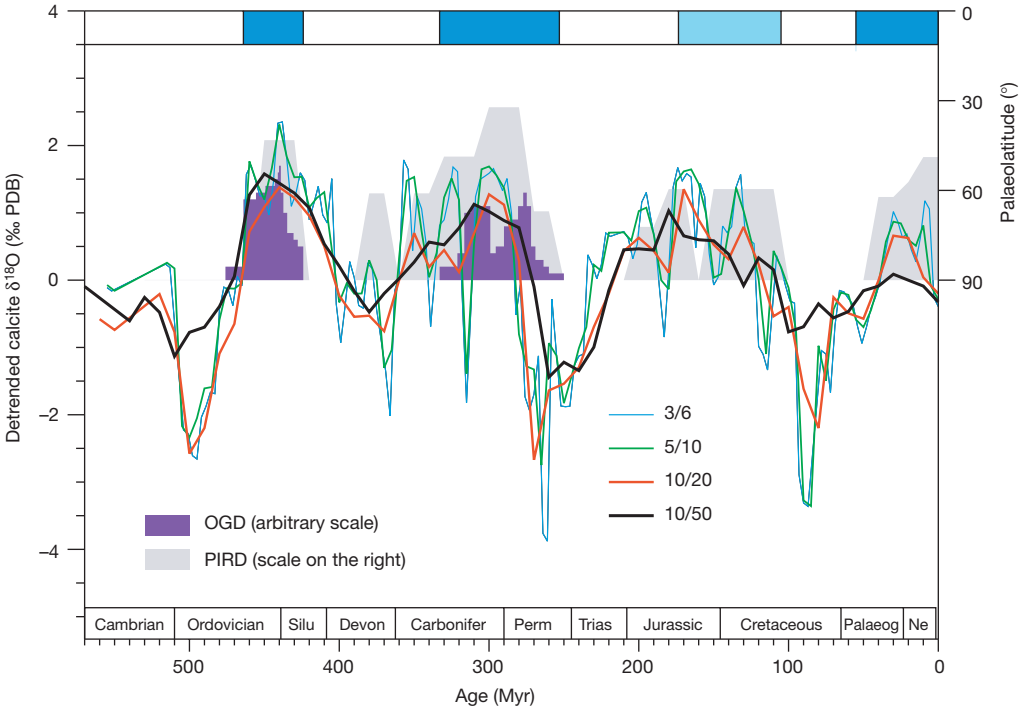

Figure 1 Detrended running means of $\delta^{18}O$ values of calcitic shells for the Phanerozoic. Detrending was achieved by subtracting the least-squares linear fit from the original data. 3/6, 5/10, 10/20 and 10/50 indicate running means at various temporal resolutions: for example, 3/6 means step 3 Myr, window 6 Myr. The palaeolatitudinal distribution of ice-rafted debris (PIRD)[22] is on the right-hand vertical axis. The frequency histograms of other glacial deposits (OGD)—such as tillites and glacial marine strata—for pre-Triassic times[1] are dimensionless. The blue bars at the top represent cool climate modes (icehouses) and the white bars the warm modes (greenhouses), as established from sedimentological criteria[1]. The lighter blue shading for the Jurassic/Cretaceous icehouse reflects the fact that true polar ice caps have not been documented for this time interval.

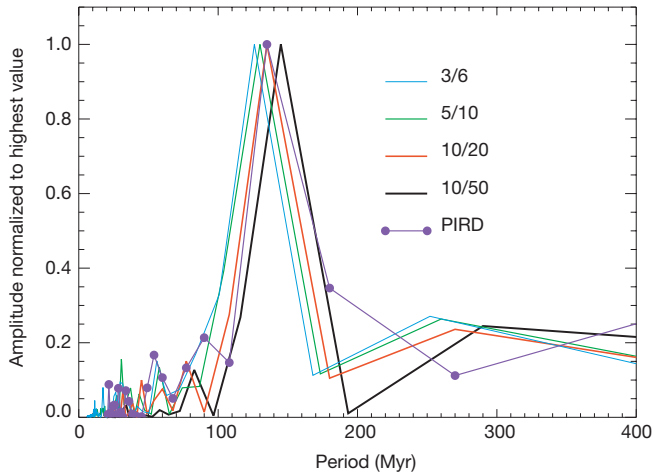

Figure 2 Periodogram of the Fourier series decomposition of the detrended $\delta^{18}O$ signal and of palaeolatitudes of ice-rafted debris (PIRD). See Fig. 1 for explanations of 3/6 to 10/50. The PIRD result is based on 10 Myr interpolation. The curves are normalized to 1 for the highest value.

available only for the Ordovician/Silurian and Permo/Carboniferous glaciations[1] (Fig. 1).

From the above statistical study, we conclude that the observed oscillations of the detrended $\delta^{18}O$ signal are of climatic origin and reflect seawater temperatures. Because of the detrending, we shall discuss below the relative temperature deviations from the norm, and not the absolute temperatures.

Depending on temporal resolution, the detrended $\delta^{18}O$ oscillations have a magnitude of ~3 to ~5‰ between peaks of greenhouse and icehouse climates (Fig. 1). The coarser the resolution, the less the magnitude of the peaks. The greenhouse/icehouse oscillations of ~3‰ would indicate temperature variations of ~13 °C. However, some of this 3‰ range may be due to an ice-volume effect. Assuming no ice caps at the peaks of greenhouse climates, and assuming ice sheets of twice the present-day size for the peaks of icehouse climates, the ice-volume effect may account for about 2‰ of this range[9,24], thus reducing the actual temperature oscillations to only ~4.5 °C. Yet, the 3‰ is a reduced amplitude at 10/50 Myr resolution. By analogy with the Quaternary period, the ice effect influences seawater $\delta^{18}O$ on much shorter timescales and an amplitude of ~4‰ for the $\delta^{18}O$ (carbonate) is thus a more realistic estimate, a proposition clearly supported by the 3/6 to 10/20 curves (Fig. 1). If so, the residual after allowing for the ice-volume effect would still be ~2‰, or some 9 °C.

The above interpretation of experimental data sheds some light on two issues that are at present subject to debate. (1) Most samples in the databases[17] originate from shallow-water habitats of low-latitude, mostly palaeotropical seas. We therefore suggest that we are dealing with marked temperature variations that were of global nature and not solely events of higher latitudes. This assertion is in accord with the proposed stadial/interstadial tropical SST variations of 4–5 °C indicated by Quaternary proxy data[9–13], as well as with the stadial/interstadial $\delta^{18}O$ pattern within the Ordovician/Silurian icehouse (Fig. 15 in ref. 17). (2) The $\delta^{18}O$-based tropical palaeotemperatures disagree with palaeotemperatures predicted from atmospheric pCO_2, the latter reconstructed from carbon isotope data for palaeosols and from the stomatal index of fossil leaves (compilations in ref. 20). All these reconstructions show high pCO_2 before 350 Myr ago, a marked decrease during the Permo/Carboniferous glaciations, high values in the Mesozoic, and a final decline through Cenozoic times. We have used these reconstructions of atmospheric CO_2 as an input for an energy-balance climate model[18]. This model incorporates changes in palaeogeography, as well as the slow increase of about 5% in the solar constant during the Phanerozoic[25]. For the present-day configuration, and a doubling of atmospheric CO_2, the model produces an increase in the global mean temperature of 2.8 °C; this is at the lower end of the range of climate sensitivity to CO_2. The IPCC 1995 report[26] gives a sensitivity of 2.8–5.2 °C for the atmosphere-only models, but a higher sensitivity would only compound the difficulties mentioned below. The simulations based on such a climate model yield temperatures that are in serious disagreement with the $\delta^{18}O$-scaled tropical temperatures, particularly during Ordovician/Silurian and Jurassic/Cretaceous times. At these, mostly icehouse, times, the model simulations show tropical SSTs that were about 5 ± 1 °C warmer than the present-day value, while the $\delta^{18}O$-scaled SSTs were colder by about 2.5 °C (Fig. 3) than the Phanerozoic norm. It is the latter that are in much better agreement with geological observations.

We note that the progressive ^{18}O depletion with age in the course of the Phanerozoic (Fig. 13 in ref. 17) has been claimed to be a reflection of: (1) increasing post-depositional alteration[27]; (2) stratified oceans due to formation of warm, saline, deep waters[28]; and (3) advancing cooling of the oceans[29]. These arguments have been discussed in detail, and discounted, in ref. 17. Nevertheless, and leaving aside these counter arguments, we consider that (1)–(3) above are not the cause of the effects that we report here. For a post-depositional trend (1), the magnitude of the greenhouse/icehouse $\delta^{18}O$ oscillations would have to be inherited from the original anomalies. As these would be diminished in the course of alteration, the original anomalies would have to have been even larger than the observed ones, thus only compounding the problem. The alternative (2) would preferentially be associated with warm episodes, as opposed to glacial times, and for the Ordovician could account for no more than ~0.9‰ ^{18}O depletion in surface waters[28]. Finally, for alternative (3), one-half of the entire trend would have to be generated by progressive cooling if the Ordovician $\delta^{18}O$-scaled temperatures were to match the results of the energy-balance model. Yet, the same assumption would also generate Cambrian and Devonian tropical SSTs respectively 27 and 12 °C warmer than the Phanerozoic mean, and analogous problems would arise

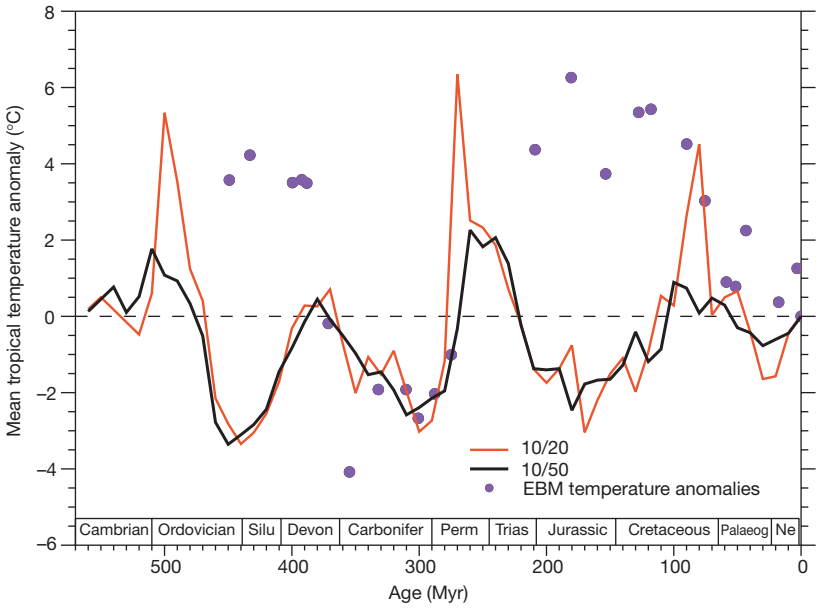

Figure 3 Tropical surface palaeotemperature anomalies calculated by the energy-balance climate model, and sea surface temperatures (SSTs) inferred from the $\delta^{18}O$ data. Filled circles, model predictions; red and black lines, SSTs calculated assuming the existence of ice sheets of twice the present-day size at the peaks of icehouse climates, with sea water $\delta^{18}O$ scaled to –0.7‰ SMOW at times with no ice caps. The palaeothermometer of ref. 30 is applied, assuming that the detrended baseline seawater $\delta^{18}O$ value is 0‰ SMOW. Further explanations as in Fig. 1.

before, and following, the Jurassic/Cretaceous icehouse. Considering the similarity of faunal assemblages, in our case brachiopods, this is an unpalatable proposition[17].

Three possible implications of our findings are: (1) the reconstructed past CO_2 levels are (partially) incorrect; (2) the role of pCO_2 as the main driving force of past global (long-term) climate changes is questionable, at least during two of the four main cool climate modes of the Phanerozoic; and (3) climate models, which include numerous parametrizations, are calibrated to the present (an interstadial in an icehouse climate), and may thus be unable to reproduce correctly the past climate modes. We hope that our results will stimulate further work on these three issues. □

Received 7 July; accepted 2 October 2000.

1. Frakes, L. A., Francis, J. E. & Syktus, J. I. *Climate Modes of the Phanerozoic* (Cambridge Univ. Press, Cambridge, 1992).
2. Fischer, A. G. in *Climate in Earth History* (eds Berger, W. H. & Crowell, J. C.) 97–104 (Natl Acad. Sci., Washington DC, 1982).
3. Worsley, T. R., Nance, R. D. & Moody, J. B. Tectonic cycles and the history of the Earth's biogeochemical and paleoceanographic record. *Paleoceanography* **1,** 233–263 (1986).
4. Steiner, J. & Grillmair, E. Possible galactic causes for periodic and episodic glaciations. *Geol. Soc. Am Bull.* **84,** 1003–1018 (1973).
5. Williams, G. E. Possible relation between periodic glaciation and the flexure of the galaxy. *Earth Planet. Sci. Lett.* **26,** 361–369 (1975).
6. Hays, J. D., Imbrie, J. & Shackleton, N. J. Variations in the Earth's orbit: pacemaker of the ice ages. *Science* **194,** 1121–1132 (1976).
7. Crowley, T. J. Pleistocene temperature changes. *Nature* **371,** 664 (1994).
8. Broecker, W. S. Glacial climate in the tropics. *Science* **272,** 1902–1904 (1996).
9. Guilderson, T. P., Fairbanks, R. G. & Rubenstone, J. L. Tropical temperature variations since 20,000 years ago: modulating interhemispheric climate change. *Science* **263,** 663–665 (1994).
10. Stute, M. *et al.* Cooling of tropical Brazil (5°C) during the last glacial maximum. *Science* **269,** 379–383 (1995).
11. Rind, D. & Peteet, D. Terrestrial conditions at the last glacial maximum and CLIMAP sea-surface temperature estimates: are they consistent? *Quat. Res.* **24,** 1–22 (1985).
12. Thompson, L. G. *et al.* Late glacial stage and Holocene tropical ice core records from Huascarán, Peru. *Science* **269,** 46–50 (1995).
13. Beck, J. W., Récy, J., Taylor, F., Edwards, R. L. & Gabioch, G. Abrupt changes in early Holocene tropical sea surface temperature derived from coral records. *Nature* **385,** 705–707 (1997).
14. CLIMAP Project Members *Map and Chart Series MC-36* (Geological Society of America, Boulder, Colorado, 1981).
15. Bush, A. B. G. & Philander, S. G. H. The role of ocean-atmosphere interactions in tropical cooling during the Last Glacial Maximum. *Science* **279,** 1341–1344 (1998).
16. Crowley, T. J. Climate SSTs re-visited. *Clim. Dyn.* **16,** 241–255 (2000).
17. Veizer, J. *et al.* $^{87}Sr/^{86}Sr$, $\delta^{13}C$ and $\delta^{18}O$ evolution of Phanerozoic seawater. *Chem. Geol.* **161,** 59–88 (1999).
18. François, L. M. & Walker, J. C. G. Modelling the Phanerozoic carbon cycle and climate: constraints from the $^{87}Sr/^{86}Sr$ isotopic ratio of seawater. *Am. J. Sci.* **292,** 81–135 (1992).
19. Berner, R. A. GEOCARB II: a revised model for atmospheric CO_2 over Phanerozoic time. *Am. J. Sci.* **294,** 56–91 (1994).
20. Berner, R. A. The carbon cycle and CO_2 over Phanerozoic time: the role of land plants. *Phil. Trans. R. Soc. Lond. B.* **353,** 75–82 (1998).
21. Gibbs, M. T., Bice K. L., Barron, E. J. & Kump, L. R. in *Warm Climates in Earth History* (eds Huber, B. T., MacLeod, K. G. & Scott, L. W.) 386–422 (Cambridge Univ. Press, Cambridge, 2000).
22. Frakes, L. A. & Francis, J. E. A guide to Phanerozoic cold polar climates from high-latitude ice-rafting in the Cretaceous. *Nature* **333,** 547–549 (1988).
23. Harland, W. B. *et al. A Geologic Timescale* (Cambridge Univ. Press, Cambridge, 1990).
24. Savin, S. M. The history of the earth's surface temperature during the past 100 million years. *Annu. Rev. Earth Planet. Sci.* **5,** 319–355 (1977).
25. Endal, A. S. & Sofia, S. Rotation in solar-type stars, I, Evolutionary models for the spin-down of the sun. *Astrophys. J.* **243,** 625–640 (1981).
26. Houghton, J. T., Meira Filho, L. G., Callander, B. A., Kattenberg, A. & Maskell, K. (eds) *Climate Change 1995: The Science of Climate Change* (Cambridge Univ. Press, Cambridge, 1996).
27. Degens, E. T. & Epstein, S. Relationship between $^{18}O/^{16}O$ ratios in coexisting carbonates, cherts and dolomites. *Am. Ass. Petrol. Geol. Bull.* **46,** 534–542 (1962).
28. Railsback, LB. Influence of changing deep ocean circulation on the Phanerozoic oxygen isotopic record. *Geochim. Cosmochim. Acta* **54,** 1501–1509 (1990).
29. Knauth, L. P. & Epstein, S. Hydrogen and oxygen isotope ratios in nodular and bedded cherts. *Geochim. Cosmochim. Acta* **40,** 1095–1108 (1976).
30. Hays, P. D. & Grossman, E. L. Oxygen isotopes of meteoric calcite cements as indicators of continental paleoclimate. *Geology* **19,** 441–444 (1991).

Acknowledgements

This work was supported by the Deutsche Forschungsgemeinschaft (Leibniz Prize and research grants to J.V.) and by the Natural Sciences and Engineering Research Council of Canada. International cooperation was facilitated by the Canadian Institute for Advanced Research (Toronto), with support from NORANDA and Hatch Investments Ltd. Y.G. and L.M.F. were supported by the Belgian National Foundation for Scientific Research (FNRS).

Correspondence and requests for materials should be addressed to J.V. (e-mail: veizer@science.uottawa.ca).

Evidence from Sardinian basalt geochemistry for recycling of plume heads into the Earth's mantle

D. Gasperini*†, J. Blichert-Toft*, D. Bosch‡, A. Del Moro§, P. Macera†, P. Télouk* & F. Albarède*

* *Ecole Normale Supérieure, 69364 Lyon Cedex 07, France*
† *Dipartimento di Scienze della Terra, Universita' degli Studi di Pisa, Via S. Maria, 53, 56126 Pisa, Italy*
‡ *Université Montpellier 2, 34095 Montpellier Cedex 05, France*
§ *Istituto di Geocronologia e Geochimica Isotopica, CNR, Via Alfieri, 1, 56010 Ghezzano-Pisa, Italy*

Up to 10 per cent of the ocean floor consists of plateaux[1]—regions of unusually thick oceanic crust thought to be formed by the heads of mantle plumes. Given the ubiquitous presence of recycled oceanic crust in the mantle source of hotspot basalts, it follows that plateau material should also be an important mantle constituent. Here we show that the geochemistry of the Pleistocene basalts from Logudoro, Sardinia, is compatible with the remelting of ancient ocean plateau material that has been recycled into the mantle. The Sr, Nd and Hf isotope compositions of these basalts do not show the signature of pelagic sediments. The basalts' low CaO/Al_2O_3 and Ce/Pb ratios, their unradiogenic ^{206}Pb and ^{208}Pb, and their Sr, Ba, Eu and Pb excesses indicate that their mantle source contains ancient gabbros formed initially by plagioclase accumulation, typical of plateau material. Also, the high Th/U ratios of the mantle source resemble those of plume magmas. Geochemically, the Logudoro basalts resemble those from Pitcairn Island, which contain the controversial EM-1 component that has been interpreted as arising from a mantle source sprinkled with remains of pelagic sediments[2,3]. We argue, instead, that the EM-1 source from these two localities is essentially free of sedimentary material, the geochemical characteristics of these lavas being better explained by the presence of recycled oceanic plateaux. The storage of plume heads in the deep mantle through time offers a convenient explanation for the persistence of chemical and mineralogical layering in the mantle.

Variations of $\delta^{18}O$ in Hawaiian basalts indicate that their mantle source contains material that was once exposed to alteration at low to medium temperatures. The positive correlation between $\delta^{18}O$ and the $^{187}Os/^{188}Os$ ratio for the different Hawaiian volcanoes strongly suggests that the component altered at the lowest temperature (Koolau) has the largest time-integrated Re/Os ratio and therefore represents the upper layers of an ancient oceanic crust[4]. The other end-member of this correlation (Mauna Kea) was identified with the lower gabbroic oceanic crust, a conjecture strongly supported by the discovery of Sr anomalies in melt inclusions from Mauna Loa lavas[5]. In addition, the rather radiogenic Hf in the Koolau component and the curvature of the Hf–Pb isotope correlation for Hawaiian volcanoes require the presence of ancient pelagic sediments in the source of Hawaiian basalts[6].

More components have been identified in the source of other hotspot basalts. The large U/Pb ratio ('HIMU'; that is, 'high μ', where $\mu = {}^{238}U/{}^{204}Pb$) characteristic of St Helena and some Polynesian basalts has been ascribed to the presence of ancient sea-floor basalts depleted in Pb and enriched in seawater U by hydrothermal activity[3]. Yet other hotspots, such as Pitcairn, contain a more controversial component (EM-1) that has some trace-element and isotope characteristics reminiscent of pelagic and/or metalliferous sediments[2,3]. Alternatively, EM-1 has been compared with melts from the subcontinental lithospheric mantle (see discussion in ref. 7). Because of its nearly ubiquitous character in ocean island